Studying charge-trapping defects within the silicon lattice of a p-channel CCD using a single-trap "pumping" technique.

Journal Item

Preprint typeset in JINST style - HYPER VERSION

Studying charge-trapping defects within the silicon lattice of a p-channel CCD using a single-trap "pumping" technique

D. Wood[a]*, D.J. Hall[a], N.J. Murray[a], J.P.D. Gow[a], A. Holland[a], P. Turner[b] and D. Burt[b]

[a] *Centre for Electronic Imaging,*
The Open University, Walton Hall, Milton Keynes, MK76AA, UK
[b] *e2v Technologies Plc,*
Chelmsford, Essex, UK
E-mail: daniel.wood@open.ac.uk

ABSTRACT: The goals of future space missions such as Euclid require unprecedented positional accuracy from the responsible detector. Charge coupled devices (CCDs) can be manufactured with exceptional charge transfer properties; however the harsh radiation environment of space leads to damage within the silicon lattice, predominantly through proton collisions. The resulting lattice defects can trap charge, degrading the positional accuracy and reducing the useful operating time of a detector. Mitigation of such effects requires precise knowledge of defects and their effects on charge transfer within a CCD. We have used the technique of single-trap "pumping" to study two such charge trapping defects; the silicon divacancy and the carbon interstitial, in a p-channel CCD. We show this technique can be used to give accurate information about trap parameters required for radiation damage models and correction algorithms. We also discuss some unexpected results from studying defects in this way.

KEYWORDS: CCD, silicon, defect, radiation damage, p-channel, pocket pumping, Euclid.

*Corresponding author.

Contents

1. Introduction

The long-term effects of radiation damage on any semiconductor material detector can be separated into two distinct classes; surface damage effects resulting from ionization as an impinging particle passes through the detector, and bulk damage effects which occur due to displacement damage within the semiconductor lattice [1]. Surface damage leads to increased dark signal and can cause flat-band voltage shifts and leakage currents within the detector [2], whilst displacement damage leads to the formation of stable lattice defects which can produce mid-band gap energy levels that degrade detector charge transfer performance [3].

For the case of scientific CCDs surface effects are largely negated by physical radiation hardening of the device and the ability to operate with the silicon surface inverted; causing holes (for n-channel devices) or electrons (for p-channel devices) from the column stops to migrate to the Si/SiO_2 interface and suppress dark current generation [4]. Bulk effects can also cause dark current increase, however the focus of this paper is the degradation of charge-transfer efficiency (CTE) by the induced lattice defects; if left unaddressed this can significantly reduce the useful operating time of a CCD.

The degradation of CTE can be mitigated through the use of iterative post-image correction algorithms which simulate charge capture and release by defect energy levels [5]. The accuracy of the model and hence the success of the correction depends on detailed knowledge of the defect parameters; ideally we wish to know exactly the length of time between the capture and emission of a signal electron (n-channel) or hole (p-channel) at the defect level, which corresponds to the emission time constant of the defect.

CCDs are increasingly required for very precise measurements; for example the ESA Euclid visible imager (VIS) instrument will aim to study subtle gravitational lensing effects through shape measurements of approximately 1.5 billion galaxies [6][7]. The VIS focal plane will be composed of 36 n-channel CCDs; at present n-channel devices can be produced which exhibit greater CTE and suffer from less dark current generation than comparable p-channel devices [8]. However it is believed that for future long-term space missions p-channel CCDs could represent a more radiation-hard alternative to traditional n-channel devices, since the radiation induced hole-capturing defect levels in a p-channel device may not have such a significant detrimental effect on CTE as the electron-capturing levels in an n-channel device at the typical operating temperatures and timings of such missions [8]. To this end, we are here analysing defects within a p-channel CCD with a view to use of this technology in future scientific applications. Gravitational lensing measurements will require highly detailed knowledge of the detector point spread function (PSF) and accurate models of the effects of radiation damage on the PSF [9]. In this paper we use the technique of trap pumping [10][11][12][13][14] with a p-channel e2v CCD 204 [15] to analyse charge-trapping defects individually, with the aim of providing accurate information about defect emission time constants for the improvement of radiation damage models and CTE degradation correction algorithms.

2. Charge-Trapping

The capture (recombination) and release (generation) of charge carriers at mid-band gap deep levels is described by Shockley-Read-Hall (SRH) kinetics, which equates generation and recombination rates to form differential equations describing carrier concentrations [16][17]. The electron/hole capture rates at a defect are given by Equations 2.1 and 2.2 where n and p are the electron and hole densities respectively, v_{th} is the thermal velocity of the carriers, and $\sigma_{n,p}$ are the cross-sections for electrons and holes.

$$c_n = n\sigma v_{th}\,, \tag{2.1}$$

$$c_p = p\sigma v_{th}\,, \tag{2.2}$$

Under steady state conditions Equations 2.3 and 2.4 give the relationship between capture and emission rates, where n_T and p_T are the SRH densities shown in Equations 2.5 and 2.6 which give the carrier concentrations when the Fermi level E_F coincides with the defect energy level E_T in terms of N_c and N_v; the densities of states in the conduction band and valence band respectively.

$$e_n = c_n n_T\,, \tag{2.3}$$

$$e_p = c_p p_T\,, \tag{2.4}$$

$$n_T = N_c exp(-\frac{E_c - E_T}{kT})\,, \tag{2.5}$$

$$p_T = N_v exp(-\frac{E_T - E_v}{kT})\,, \tag{2.6}$$

The above expressions for capture and emission rates lead to Equations 2.7 and 2.8 describing the capture and emission time constants for a defect of energy E_T above the valence band edge (shown for p-channel only since that is the concern of this paper):

$$\tau_c = \frac{1}{p\sigma v_{th}}, \tag{2.7}$$

$$\tau_e = \frac{1}{N_v \sigma v_{th}} exp(\frac{E_T}{kT}), \tag{2.8}$$

In this paper we use the method of trap pumping to investigate defect emission time constants and their temperature dependence over a small range, with a view to a much larger silicon lattice defect study in the near future. There are a vast number of possible stable defects within the silicon lattice, however in this paper we focus on two of those that are known to cause CTE degradation in p-channel CCDs under typical operating conditions: the silicon divacancy and the carbon interstitial.

3. Trap Pumping

Trap pumping works by altering the sequence of the clock phase electrodes within a CCD such that a signal charge packet is moved back and forth between two adjacent pixels many times (the number of pumping cycles N)[13][14]. Both the image section and serial register of a CCD can be pumped. Moving charge in this way amplifies the effects of any charge trapping defects within a pixel. Starting with a flat-field exposure the signal is pumped for N cycles and then read out normally. During each pumping cycle there exists a probability that a defect may capture a signal charge from the charge packet within a given pixel and then release it into an adjacent pixel. Repeating the cycle many times leads to characteristic dipoles within the resulting image at defect locations, such as those shown in Figure 1.

The capture and emission time constants can be used to model the trapping process and obtain an expression for the dipole intensity. A full explanation of the trap pumping process is outlined in [10]. To a first approximation we can assume that if a charge carrier comes into contact with an empty trap the capture is instant (in other words τ_c is negligible compared to τ_e) leading to Equation 3.1 which describes for a 3-phase CCD the probability per cycle that a given electron is pumped in terms of the period of time for which a charge packet resides beneath a single phase electrode; the "phase time", t_{ph}:

$$P_p = exp\left(\frac{-t_{ph}}{\tau_e}\right) - exp\left(\frac{-2t_{ph}}{\tau_e}\right) \tag{3.1}$$

The e2v CCD204 is in fact a 4-phase device, however for the duration of this study two of the phases were connected together such as to clock the CCD as a 3-phase device. If it is assumed that the probability of capture is 100% (providing the trap is empty) then the dipole intensity I is given to a first approximation by $I = NP_p$ for N pumping cycles. If the capture probability is not 100% then the intensity is scaled approximately linearly with P_c where P_c is the capture probability for a given signal level.

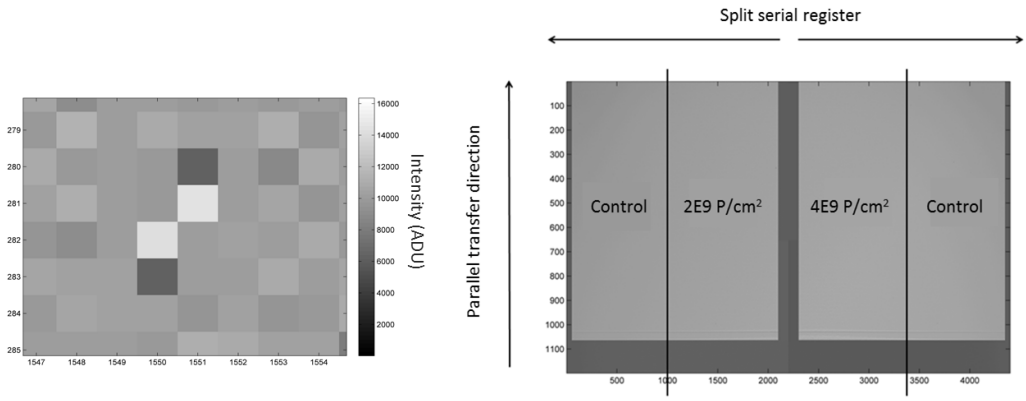

Figure 1: Left - Characteristic dipoles produced in a trap pumped image taken from the image section of the device. Each square represents one pixel. Right - Outline of the irradiated regions of the e2v CCD204. Due to the split serial register, the whole image area is reproduced by stitching together images from the left and right sections; giving the central region of overscan. Axis labels show the pixel number.

By tracking I across a range of t_{ph} which surrounds the emission time constant we produce dipole intensity curves for each defect. Differentiation of the expression for intensity shows that the curve maximum should lie at $ln(2) \times \tau_e$. Therefore we have a method of directly probing the emission time constant parameter space.

4. Experimental Results + Discussion

4.1 Identifying Dipoles

The e2v CCD204 consists of a 4k by 1k pixels image area with a split serial register. Two subsections of a CCD204 were irradiated with protons at a total fluence of 2×10^9 cm^{-2} and 4×10^9 cm^{-2} respectively, for 10 MeV equivalent protons [15] (for reference, the Euclid end of life fluence is expected to be around 5×10^9 cm^{-2})[18]. By 10 MeV equivalent fluence we refer to the fluence of 10 MeV protons which would cause the same amount of displacement damage, as indicated by the NIEL scaling hypothesis [**?**]. The outline of each irradiated region is shown in Figure 1.

A recent study by Mostek *et al.* [11] outlined three predominant charge trapping defect species for parallel transfer in proton irradiated p-channel silicon; a hole trapping level of the silicon divacancy (VV), a carbon interstitial (C_i) and a carbon/oxygen interstitial(C_iO_i). Using a method of trap pumping in the temperature domain Mostek estimated the energy levels and cross-sections of the defect species, which can then be used to deduce emission time constants for a given temperature. The energy levels of the divacancy and carbon interstitial were found to be 0.184 ± 0.012 eV and 0.287 ± 0.068 eV above the valence band edge respectively [11]. Using the Mostek data as a guide we chose to probe the divacancy defect at temperatures of -114, -119 and -124 °C as well as the carbon interstitial at temperatures of -93, -97 and-101 °C. The reason for omission of

the carbon/oxygen interstitial from this study is that the emission time constant for that defect is many times larger than for the divacancy or carbon interstitial. The phase times required would be in the order of seconds, leading to very time consuming measurements and increased issues with accurate temperature control for the duration of each measurement. The alternative is to operate at higher temperatures, however this would lead to issues with increased dark current.

For measurements at each temperature, a flat field exposure was first taken at approximately 25000 holes intensity (equivalent to 25000 e^- intensity in an n-channel CCD) before the signal was pumped for 4000 cycles with a given phase time. Small fluctuations in the flat-field signal level do not affect the charge cloud volume within each pixel enough to have noticeable effect on the capture probability. The phase time was then increased so as to probe the time constant parameter space. To ensure that dipoles were correctly identified, first a background signal subtraction was taken from each adjacent pair of pixels and then the intensity differences for each pair were calculated. A threshold was set such that only sufficiently intense (>500 h+) dipoles were further analysed. A number of subsequent checks were then made to reduce the number of false positives, where noise or the cumulative effects of multiple defects could lead to over-estimation of defect densities.

An area of 1000 rows by 500 columns was analysed for both irradiated regions as well as a control region. Table 1 gives the estimated defect density values for each defect species in both irradiated sections of the device as well as the control section, where each density value is an average of the number of defects across the three corresponding temperatures. These values do not relate to the true number of defects within the lattice but instead the number that can be assumed to interact with a signal charge cloud of this size (25000 h+). Density values have also been doubled since the method of trap pumping only reveals defects beneath barrier phase-electrodes [13]. It can be seen in Table 1 that the defect densities scale consistently with the radiation fluence.

Table 1: Trap densities for each region of the device.

	Control	2×10^9 p+cm-2	4×10^9 p+cm-2
C_i	$(1.07 \pm 0.05) \times 10^{-3}$ pix-1	$(9.22 \pm 0.15) \times 10^{-3}$ pix-1	$(1.54 \pm 0.02) \times 10^{-2}$ pix-1
VV	$(1.66 \pm 0.06) \times 10^{-3}$ pix-1	$(1.95 \pm 0.02) \times 10^{-2}$ pix-1	$(4.60 \pm 0.03) \times 10^{-2}$ pix-1

4.2 Emission Time Constants

Once dipoles were identified the intensity curves were produced and fit with a curve corresponding to Equation 3.1. Curves were fitted using the Nelder-Mead method to perform an unconstrained, non-linear minimization of the sum of squared residuals with respect to the various parameters [19]. Figure 2 shows several of the intensity curves for each defect species; it was observed that for a large number (~50%) of the carbon interstitial defects the intensity curve was inverted such that the emission time constant is proportional to the phase time at a minimum of the curve rather than a maximum. This did not appear to affect the time constants themselves; τ_e values calculated from the inverted curves are distributed equally with those calculated from the regular curves. However the inversion of the intensity curves was unexpected and is very intriguing since it appears that the carbon interstitial defect in each case is pumping signal in anti-phase with a flat level of pumping

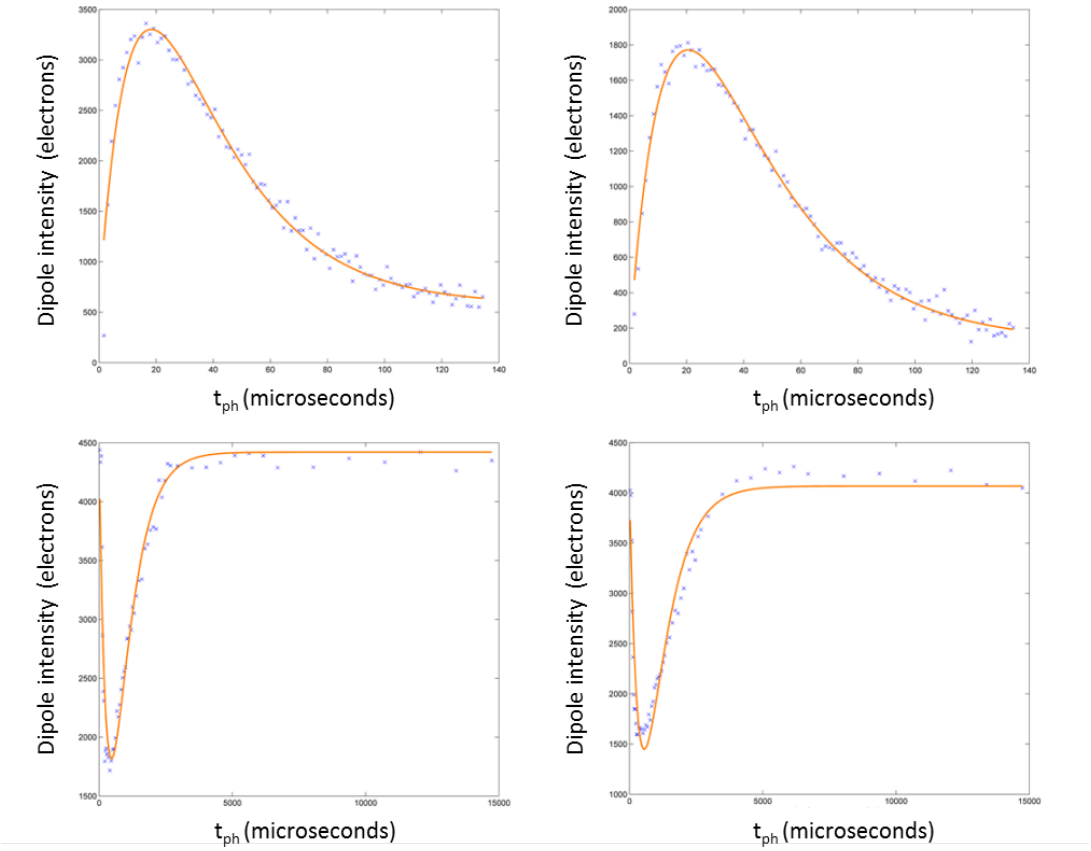

Figure 2: Examples of the intensity curves produced for dipoles by varying the phase time t_{ph}. The top two curves show the expected behaviour, whilst the bottom two show examples of the "inversion" which was observed for many of the carbon interstitial defects.

which is time independent; to the best of our knowledge, this phenomenon is previously unreported in the literature. Further study is required in this area to see if similar effects are observed in different devices. Any signal or field dependence of the flat level would also provide more information.

After fitting each intensity curve the emission time constants were obtained from the parameters of the fitted curves. For defects producing reliable curves at all three temperatures the emission time constant was plotted against temperature. To find reliable curves the Pearson correlation coefficient was used, with a lower threshold of 0.95 for the divacancy defects and 0.80 for the carbon interstitials (which in general produced less well defined intensity curves). Figure 3 shows the resulting plots for each defect species in both irradiated sections of the device, with one line representing one defect tracked across the three temperatures and the τ_e value estimated by Mostek also shown [11]. It can be seen that for both defect species the calculated emission time constants are in agreement with the values estimated in the Mostek study. Tables 2 and 3 give the mean values of τ_e as well as the standard deviation at each temperature for the divacancy and carbon defects respectively. Example histograms of the emission time constants are given in Figure 4 and

show for the divacancy defect a Gaussian distribution. Since the carbon defects are less numerous the distributions are less well defined; however they also appear to be following an approximate Gaussian distribution.

Table 2: Emission time constants and standard deviation for divacancy defects at each of the three temperatures.

	$-114°C$	$-119°C$	$-124°C$
τ_e (s)	2.12×10^{-5}	3.79×10^{-5}	6.54×10^{-5}
Spread (s)	5.20×10^{-6}	9.17×10^{-6}	1.60×10^{-5}

Table 3: Emission time constants and standard deviation for carbon interstitial defects at each of the three temperatures.

	$-93°C$	$-97°C$	$-101°C$
τ_e (s)	3.91×10^{-4}	6.65×10^{-4}	1.02×10^{-3}
Spread (s)	1.75×10^{-4}	3.16×10^{-4}	5.07×10^{-4}

4.3 Discussion

From Tables 2 and 3 and Figure 3 it is clear that there is still a large spread in τ_e; however the parallel nature of the lines for each defect appear to show that this visible spread is genuine rather than the result of measurement uncertainties. Figure 4 shows τ_e for 100 of the divacancy defects and allows for a clearer view of the distribution. We would expect some spread in the data due to the effects of nearby defects with much larger or smaller time constants, small temperature fluctuations during the pumping cycles and also because of our approximation that charge capture is instant. Other sources could include a possible Poole-Frenkel type effect where the orientation of the electric field within a given pixel would reduce the energy required for generation events [20]. We plan to test this in a further study through adjusting the clocking voltages and monitoring any effect on the spread in time constant data. Other possibilities include multiple lattice configurations of the same defect; it is well known that lattice defects are often metastable [21], however the effects of different configurations on time constants are not fully understood.

5. Conclusions

We have studied two defect species within a p-channel CCD using trap pumping. A simple model of the charge trapping process described by two exponential time constants has been utilised to obtain emission time constant data for both the divacancy hole-trapping level and the carbon interstitial. We have shown that this method can lead to improvements in our knowledge of defect emission time constants, which are extremely valuable for use in radiation damage models and correction algorithms. We have found that for the case of the carbon interstitial defect many dipole intensity curves have been inverted, showing evidence of time independent signal pumping for which there is currently no explanation. High resolution in the time constant data has also allowed

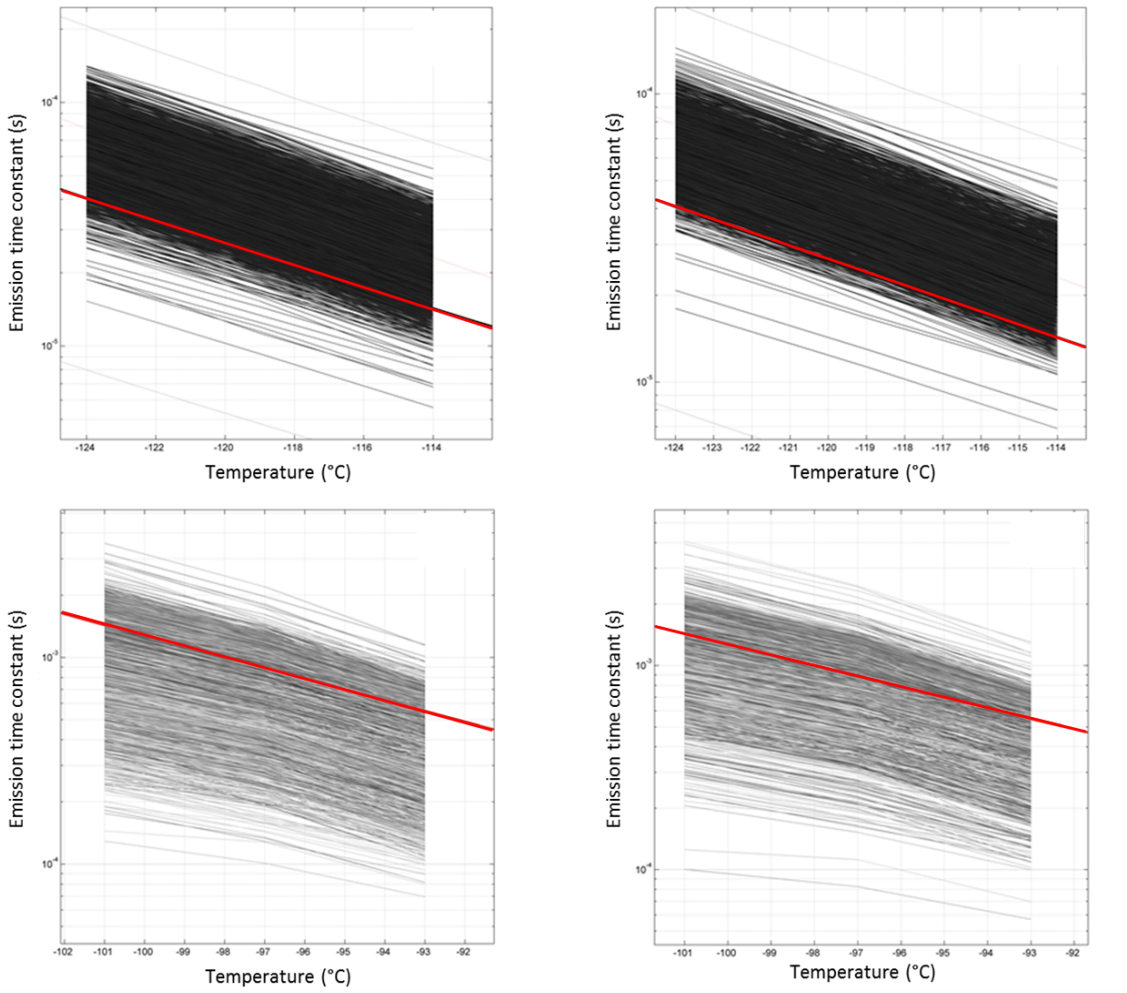

Figure 3: Clockwise from top left - Emission time constants against temperature for; 6677 divacancy defects in the heavily irradiated region, 2317 divacancy defects in the less heavily irradiated region, 911 carbon interstitial defects in the less heavily irradiated region and 1434 carbon interstitial defects in the heavily irradiated region. Each line corresponds to a single defect tracked across three temperatures (3 data points on each line). The red lines show the emission time constant of each defect as estimated using the Mostek *et al.* energies and cross-sections [11].

us to observe a large amount of apparently genuine spread which exists for τ_e. It may be that we are limited by genuine spread which could have many sources, several of which have been suggested. Further investigation into possible signal or field dependence of these effects is needed, as well as a more rigorous model of the capture process. A similar study on a much larger scale is planned for the near future using several n-channel devices both un-irradiated and after irradiations using protons, electrons, heavy ions and gamma rays. We aim to build upon the work carried out in this initial study to both provide highly accurate time constant data for relevant charge-trapping defects across a larger temperature range, as well as investigate further some of the current unknowns to

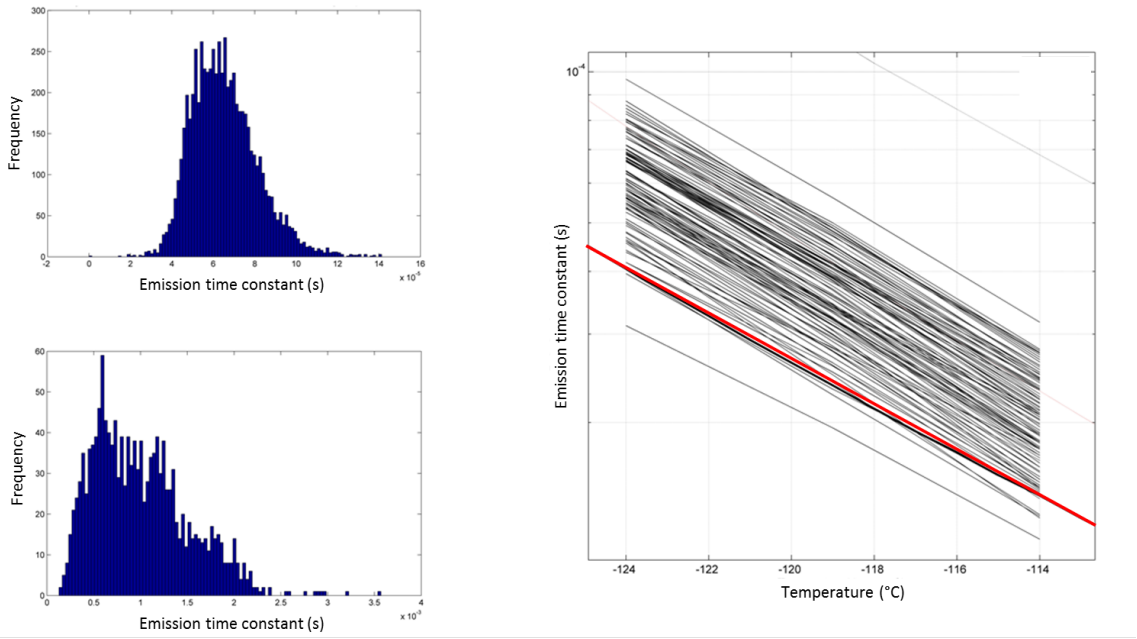

Figure 4: Left - Histograms of the emission time constants for divacancy defects at -124 °C (top) and carbon interstitial defects at -101 °C. The shape and spread of the distributions, particularly in the carbon interstitial case, are not clearly understood and will be an interesting avenue of further study once we have many more defects for analysis. Right - The emission time constant against temperature for 100 randomly selected divacancy traps, shown to outline the parallel nature of the lines for each individual defect.

build a clearer picture of the charge-trapping process. There is also the potential for the combination of this technique with a model of charge-packet volume within a CCD pixel; in order to model the number of relevant defects which will interact with a charge-packet for a given set of conditions such as signal level, radiation dose, temperature and CCD operating parameters.

Acknowledgments

With thanks to ESA for providing the devices used during this study.

References

[1] C. Dale, P. Marshall, B. Cummings, L. Shamey & A. Holland. *Displacement damage effects in mixed particle environments for shielded spacecraft CCDs*, *IEEE Transactions on Nuclear Science* **40**, 1993. doi:10.1109/23.273497

[2] G.R. Hopkinson, C.J.Dale & P.W. Marshall. *Proton effects in charge-coupled devices.*, *IEEE Transactions on Nuclear Science* **43**, Pages 614-627, 1996.

[3] J.R. Srour, C.J. Marshall & P.W. Marshall. *Review of displacement damage effects in silicon devices*, *IEEE Transactions on Nuclear Science* **50**, 2003. doi:10.1109/TNS.2003.813197

[4] J. R. Janesick, *Scientific charge-coupled devices*, Washington: SPIE - The International Society for Optical Engineering, 2001, ch. 7, pp. 632-634.

[5] R. Massey, C. Stoughton, A. Leauthaud, J. Rhodes, A. Koekemoer, R. Ellis and E. Shaghoulian. *Pixel-based correction for Charge Transfer Inefficiency in the Hubble Space Telescope Advanced Camera for Surveys*, *MNRAS* **401**, 2010.

[6] R. Laureijs *et al.* (2011, Oct). Euclid Definition Study Report, ArXiv e-prints 1110.3193 [Online]. Available: http://arxiv.org/abs/1110.3193.

[7] M. Cropper, H. Hoekstra, T. Kitching, R. Massey, J. Amiaux, L. Miller, Y. Mellier, J. Rhodes, B. Rowe, S. Pires, C. Saxton and R. Scaramella. *Defining a weak lensing experiment in space*, *MNRAS* **431**, Pages 3103-3126, 2013.

[8] J.P.D Gow, N.J. Murray, A.D. Holland, D. Burt and P.J. Pool. *Comparison of proton irradiated p-channel and n-channel CCDs*, *Nuclear Instruments and Methods in Physics Research A* **686** Pages 15-19, 2012.

[9] D.H. Weinberg, M.J Mortonson, D.J. Eisenstein, C. Hirata, A.G. Riess & E. Rozo. *Observational Probes of Cosmic Acceleration*, *Physics Reports* **530**, Issue 2, Pages 87-255, 2013.

[10] D. Hall, N.Murray, A. Holland, J. Gow, A. Clarke and D. Burt. *Determination of In Situ Trap Properties in CCDs Using a "Single-Trap Pumping" Technique*, *IEEE Transactions on Nuclear Science* **61** Pages 1826-1833, 2014.

[11] N. J. Mostek, C. J. Bebek, A. Karcher, W. F. Kolbe, N. A. Roe and J. Thacker. *Charge trap identification for proton-irradiated p+ channel CCDs*, *Proc. SPIE* **7742**, 2010.

[12] J. R. Janesick, "Charge transfer" in *Scientific charge-coupled devices*, Washington: SPIE - The International Society for Optical Engineering, 2001, ch. 5, sec. 5.3.4, pp. 430-433.

[13] N. J. Murray, A. D. Holland, J. P. D. Gow, D. J. Hall, J. H. Tutt, D. Burt and J. Endicott. *Mitigating radiation-induced charge transfer inefficiency in full-frame CCD applications by 'pumping' traps*, *Proc. SPIE* **8453** pp. 845317, 2012.

[14] N. J. Murray, D. J. Burt, D. Hall and A. D. Holland. *The relationship between pumped traps and signal loss in buried channel CCDs*, *Proc. SPIE* **8860**, 2013.

[15] J.P.D Gow, N.J. Murray, A.D. Holland & D. Burt *Proton damage comparison of an e2v technologies n-channel and p-channel CCD204*, *IEEE Transactions on Nuclear Science* **61**, 2014. doi:10.1109/TNS.2014.2298254

[16] W. Shockley and W. T. Read Jr. *Statistics of the recombinations of holes and electrons*, *Phys. Rev.* **87** no. 5, pp. 835-842, 1952.

[17] R. N. Hall, *Electron-hole recombination in germanium*, *Phys. Rev.* **87** no.5, pp.387, 1952.

[18] J.P.D Gow, N.J. Murray, D.J. Hall *et al.*, *Assessment of proton radiation-induced charge transfer inefficiency in the CCD273 detector for the Euclid dark energy mission*, *Proc. SPIE* vol.8453, 2012.

[19] J.C. Lagarias, J.A. Reeds, M.H. Wright and P.E. Wright. *Convergence properties of the Nelder-Mead simplex method in low dimensions*, *SIAM Journal of Optimization* **9**, Pages 112-147, 1998.

[20] J. Frenkel, *On pre-breakdown phenomena in insulators and electronic semi-conductors*, *Phys. Review* **54**, 1938.

[21] R. Pinacho, P. CAstrillo, M. Jaraiz, I. Martin-Bragado, J. Barbolla, H.J. Gossmann and J.L. Benton. *Carbon in silicon: Modelling of diffusion and clustering mechanisms*, *Journal of Applied Physics* **92**, 2002.